Loss of ZIP facilitates JAK2-STAT3 activation in tamoxifen-resistant breast cancer

Ning Zhu[a,b,c,d], Jing Zhang[d], Yuping Du[b], Xiaodong Qin[d], Ruidong Miao[b], Jing Nan[b,e], Xing Chen[e], Jingjie Sun[b], Rui Zhao[b], Xinxin Zhang[f], Lei Shi[b], Xin Li[b], Yuxi Lin[b], Wei Wei[b], Aihong Mao[g,h], Zhao Zhang[i], George R. Stark[e,1], Yuxin Wang[e,1], and Jinbo Yang[a,b,f,1]

[a]Key Laboratory of Marine Drugs, Chinese Ministry of Education, School of Medicine and Pharmacy, Ocean University of China, Qingdao 266003, Shandong, People's Republic of China; [b]Institute of Cancer Biology & Drug Screening, School of Life Sciences, Lanzhou University, Lanzhou 730000, Gansu, People's Republic of China; [c]Lester and Sue Smith Breast Center, Baylor College of Medicine, Houston, TX 77030; [d]State Key Laboratory of Veterinary Etiological Biology, Lanzhou Veterinary Research Institute, Chinese Academy of Agriculture Science, Lanzhou 730000, Gansu, People's Republic of China; [e]Department of Cancer Biology, Lerner Research Institute, Cleveland Clinic Foundation, Cleveland, OH 44195; [f]Innovation Center for Marine Drug Screening & Evaluation, Qingdao National Laboratory for Marine Science and Technology, Qingdao 266003, Shandong, People's Republic of China; [g]Department of Translational Medicine, Gansu Provincial Cancer Hospital, Lanzhou 730000, Gansu, People's Republic of China; [h]Center of Medical Molecular Biology, Gansu Provincial Academic Institute for Medical Research, Lanzhou 730000, Gansu, People's Republic of China; and [i]Department of Molecular Medicine, Mays Cancer Center, The University of Texas Health Science Center at San Antonio, San Antonio, TX 77229

Contributed by George R. Stark, April 22, 2020 (sent for review June 25, 2019; reviewed by Jacqueline F. Bromberg and John J. O'Shea)

Tamoxifen, a widely used modulator of the estrogen receptor (ER), targets ER-positive breast cancer preferentially. We used a powerful validation-based insertion mutagenesis method to find that expression of a dominant-negative, truncated form of the histone deacetylase ZIP led to resistance to tamoxifen. Consistently, increased expression of full-length ZIP gives the opposite phenotype, inhibiting the expression of genes whose products mediate resistance. An important example is *JAK2*. By binding to two specific sequences in the promoter, ZIP suppresses *JAK2* expression. Increased expression and activation of JAK2 when ZIP is inhibited lead to increased STAT3 phosphorylation and increased resistance to tamoxifen, both in cell culture experiments and in a mouse xenograft model. Furthermore, data from human tumors are consistent with the conclusion that decreased expression of ZIP leads to resistance to tamoxifen in ER-positive breast cancer.

tamoxifen resistance | JAK/STAT | ZIP | VBIM

Expressed in more than 70% of clinical samples, estrogen receptor α (ERα) is an important marker for breast tumor diagnosis and prognosis (1, 2). Upon estrogen binding, ERα is phosphorylated to form homo- or heterodimers (with ERβ), which recognize consensus sequences in the promoters of responsive genes, recruiting coactivators or corepressors and thus regulating transcription (3, 4). This process is crucial for the progression of the majority of primary breast tumors by regulating many genes that play important roles in cell proliferation and survival. Thus, selective estrogen receptor modulators, such as tamoxifen, have been used widely to treat ERα-dependent tumors. However, ERα expression and activity tend to be low in highly aggressive or endocrine therapy–resistant breast cancer cells (5–7). The balance between growth factor receptor and ERα expression and activation is critical for the survival of these cells (8).

The JAK-STAT pathway plays a pivotal role in transducing signals from the cell surface to target genes in response to cytokines such as IFN-α, IFN-β, IFN-γ, and interleukins and growth factors such as EGF, PDGF, growth hormone, GM-CSF, and G-CSF (9). STAT3 is an important oncogene that is constitutively activated in many types of tumors, including those of the breast (10). By promoting the expression of target genes, activated STAT3 inhibits apoptosis, regulates the cell cycle, and induces angiogenesis (11). Importantly, the functions of STAT3 depend on the status of posttranslational modifications in addition to tyrosine phosphorylation, including lysine methylation and acetylation (12–14), which are, in turn, controlled by autocrine or paracrine stimulation of specific receptors (15). Interruption of activated JAK-STAT signaling is a very attractive approach to inhibit the growth of many different cancers (16, 17).

ZIP is a repressor of transcription that includes zinc finger, TUDOR, G-patch, and coiled-coil domains (18). In response to unknown stimuli, ZIP forms a homodimer that translocates to the nucleus (18, 19). Knocking ZIP expression down in breast cancer cells leads to dysregulated proliferation, indicating its potential role as a tumor suppressor (18). Utilizing the powerful forward genetic validation-based insertional mutagenesis (VBIM) method (20–24), we cloned an N-terminal-truncated form of ZIP (dZIP) which suppresses the activity of full-length ZIP. We now report that ZIP regulates multiple pathways that mediate resistance to endocrine therapy, including estrogen receptor expression and activity, PI3K-AKT activity, and receptor tyrosine kinase (RTK) expression. Most importantly, the expression and activation of JAK2, STAT3 tyrosine phosphorylation, and resistance to tamoxifen were all dramatically increased when ZIP expression was repressed.

Significance

Tamoxifen is beneficial in treating estrogen receptor–positive breast cancer, but resistance to this treatment eventually ensues. A method to identify mechanisms of tamoxifen resistance identified the histone deacetylase ZIP, leading to the finding that increased expression of the tyrosine kinase JAK2 is one important factor. As a result of this discovery, it may be possible to use an inhibitor of JAK2 to block the aberrant activation of STAT3 caused by ZIP deficiency to help overcome or prevent tamoxifen resistance.

Author contributions: N.Z., J.Z., G.R.S., Y.W., and J.Y. designed research; N.Z., J.Z., Y.D., X.Q., R.M., J.N., X.C., J.S., R.Z., X.Z., L.S., X.L., Y.L., W.W., and Y.W. performed research; A.M. and Z.Z. contributed new reagents/analytic tools; N.Z., J.Z., Y.D., X.Q., R.M., J.N., X.C., G.R.S., Y.W., and J.Y. analyzed data; N.Z., G.R.S., Y.W., and J.Y. wrote the paper; and A.M. collected the patient samples.

Reviewers: J.F.B., Memorial Sloan Kettering Cancer Center; and J.J.O., NIH.

The authors declare no competing interest.

Data deposition: Raw ChIP-seq (PRJNA626032) and RNA-seq (PRJNA625785) data have been deposited in Gene Expression Omnibus.

[1]To whom correspondence may be addressed. Email: starkg@ccf.org, wangy7@ccf.org, or yangjb@ouc.edu.cn.

This article contains supporting information online at https://www.pnas.org/lookup/suppl/doi:10.1073/pnas.1910278117/-/DCSupplemental.

First published June 12, 2020.

Materials and Methods

Cells and Reagents. The 293T, MCF7, T47D, ZR-75-30 (ZR), BT549, 231, 468, and derived cell lines were from ATCC. The 2FTGH, U1A, U4A, and γ2A cells were described by Watling et al. (25). All cells were maintained in Dulbecco's modified Eagle's medium supplemented with 10% fetal calf serum (Gibco), 100 U/mL penicillin, and 100 mg/mL streptomycin (Sangon Biotech). Antibodies against phospho-JAK2 (Tyr1007/1008), JAK2, phosphor-STAT3 (Tyr705), STAT3, phospho-STAT1 (Tyr-701), STAT1, phospho-STAT5 (Tyr-694), STAT5, phospho-AKT (Tyr-473), AKT, pmTOR, PTEN, p-HER2, HER2, pFGFR, pSRC, pERK, pPKA, pP65, pIKK, IKK, pIκB, Iκ B, phospho-ERα (Ser167), and ERα were from Cell Signaling Technology. Hygromycin, puromycin, and anti-FLAG were from Sigma-Aldrich. Anti-ZIP was from Abgent. Antibody against mouse IgG was from Santa Cruz. Antibodies against actin and GAPDH were from Goodhere. AZD1480 and ruxolitinib were from SelleckChem. Tamoxifen citrate was from Merck. Transfection reagents were from Qiagen or Invitrogen. The luciferase assay substrate was from Promega. General biochemical reagents were from Sangon Biotech. Restriction, ligation, and PCR enzymes were from Thermo Fisher. The EGFR inhibitor (C3327), the HER2 inhibitor, AG879, the AKT inhibitor, AZD5363, and the NFκB inhibitor, QNZ, were from APExBio.

VBIM Insertion and Colony Validation. MCF7 cells, derived from a single clone, were pretreated with tamoxifen to determine the minimum lethal dose; 11 μM were sufficient to kill most of the cells. Cells (1,000 per well) were seeded in 96-well plates and infected with 50 μL of each of the three VBIM virus suspensions overnight. The medium was replaced by complete medium, and the cells were cultured for 24 h more. To minimize the possibility that an intrinsic resistant cell would be picked, 12 μM of tamoxifen were then used to treat the control and the infected pools. After 48 h, when the cells in the control groups were all dead, the surviving cells were expanded. Every positive well contained no more than one colony, so repeated isolation of the same colony was avoided. When the resistant cells had grown to 80% confluence in six-well plates, genomic DNA was extracted and digested with EcoRI and MfeI. The DNA fragments were purified and self-ligated. Nested inverse PCR using Taq polymerase and VBIM primers followed to determine DNA sequences upstream of the integration site. The fragment was ligated into the pCR2.1 vector, transformed into DH5α competent cells, and sequenced (20). Insertion sites were analyzed using Blast and the NCBI database.

Chromatin Immunoprecipitation (ChIP) and ChIP Sequencing. To perform ChIP experiments, we utilized the EZ ChIP (Upstate) buffer system. MCF7 cells in 100 mm plates were transfected with plasmids expressing ZIP or controls, and 48 h later, 270 μL of 37% formaldehyde were added to each 10 mL of medium with swirling for 10 min. One milliliter of 10 × glycine buffer (1.25 M) was then added, and the mixture was swirled for 10 min to inactivate excess formaldehyde. The medium was then removed, and the cells were washed with ice-cold phosphate-buffered saline (PBS) twice and collected into a microfuge tube with 1 mL PBS and a mixture of proteinase inhibitors, followed by centrifugation at 700 × g at 4 °C for 4 min. Then 300 μL of lysis buffer plus proteinase inhibitors were added to suspend the cells, which were sonicated 20 times for 3 s each, with a 10 s rest each time at 50% of the maximum setting (Cole Parmer Ultrasonic Processer, model CPX130), followed by centrifugation at 14,000 × g for 10 min. Supernatant solutions were diluted in dilution buffer, 60 μL of protein G agarose were added, and the mixture was rotated at 4 °C for 1 h. The agarose was then removed by centrifuging at 3,000 × g for 1 min, and 5 μL of supernatant solution were saved at 4 °C as "input." Immunoprecipitation was performed overnight at 4 °C with 1 μg mouse IgG or anti-FLAG. Protein G agarose was then added, and the mixture was rotated for another hour. The complex was washed in sequence with low-salt, high-salt, LiCl, and Tris EDTA (TE) buffers (twice). Protein–DNA complexes were then eluted with TE elution buffer at 65 °C for 5 h to reverse the cross-links. The samples were then treated with RNase A and proteinase K. A MinElute Purification Kit (Qiagen) was utilized to purify DNA extracts, and 21 to 30 cycles of PCR were performed, using the primers listed in Dataset S1.

To perform a ChIP sequencing (ChIP-seq) analysis, DNA fragments generated from MCF7-ZIP-FLAG cells by precipitation with anti-FLAG were analyzed on the Hiseq platform. Low-quality reads, degenerative reads, adaptor reads, and short reads (<18 base pairs [bp]) were excluded. Peaks were called with model-based analysis for ChIP-seq using default parameters. We have uploaded the raw data to the Gene Expression Omnibus database. Genes were considered to be regulated by ZIP only if the *P* value (immunoprecipitation group vs. input group) was <0.05. These genes are listed in Dataset S3. More detailed experimental procedures are available from Novogene.

Luciferase Reporter Assay. Half-confluent 293T cells in six-well plates were transfected with pGL4.20-puro-vectors encoding the JAK2 promoter (wild type or containing mutations in the ZIP-binding sites) We used the forward primer 5′-GAGGGCTGGGActAGAGGGTCGCGAGAAATTTCCACTTTGTAC-3′ and the reverse primer 5′-ACCCTCTagTCCCAGCCCTCTTCAATTTCCAG-3′ to mutate the first binding site GGAggAGA at −6226 to −6219 bp (upstream from translational starting codon ATG) to GGActAGA and the forward primer 5′-GAAGGActAGAGAAAAGCTTAGTTAAGGAC-3′ and the reverse primer 5′- TTCTCTagTCCTTCCCCCTTTTTTTCCC-3′ to mutate the second binding site GGAggAGA at −5482 to −5475 bp (upstream from ATG) to GGActAGA. Underlining shows the binding sites, and the mutated nucleotides are in lowercase letters. Forty-eight hours later, the cells were split into 60 mm plates, and 5 mL of medium were added, with 2.5 μM puromycin. Before they achieved 80% confluence, the cells from each plate were split into 100 mm plates with 3.0 μM puromycin and were allowed to form colonies. After 10 d (starting from the day of transfection), tens of colonies could be seen. Single colonies were picked and transferred into 96-well plates. After adhering, the cells in each well were split into two new wells. Twenty-four hours later, the luminescence of the cells in one well was measured on a Vector3 multilabel counter (PerkinElmer). Positive colonies (in the other well) were cultured to expand them, with increasing concentrations of puromycin, up to 5.0 μM. The cells were then split into puromycin-free medium for three more passages, and 5.0 μM puromycin was again used to kill nonstably transfected cells. Then, single-cell clones that were luminescence positive were picked and utilized to evaluate the promoter-specific effects of ZIP. A vector encoding FLAG-ZIP or a control vector was transiently transfected into the candidate cells, and luminescence was measured 24 h later.

Immunoprecipitation and Western Analysis. For immunoprecipitation, cell lysates were incubated in lysis buffer (50 mM Tris·HCl, pH 8.0, 0.5% Nonidet P-40, 150 mM NaCl) for 30 min at 4 °C, with agitation three times every 10 min, followed by centrifugation at 14,000 × g for 8 min at 4 °C. Five hundred microliters of supernatant solution were incubated with specific antibodies (1 μg) overnight at 4 °C with constant swirling; 40 μL of 50% protein G agarose beads were then added with incubation for 2 h more. The beads were collected by centrifugation at 8,000 × g for 1 min at 4 °C and washed three times using the lysis buffer. The precipitated proteins were eluted by suspending the beads in 2 × sodium dodecyl sulfate/polyacrylamide gel electrophoresis (SDS/PAGE) loading buffer and then heated at 95 °C for 5 min. Protein samples from patients were extracted for Western analysis utilizing Qproteome FFPE Tissue Extraction Buffer (Qiagen). Cultured cells were lysed on ice with radio immunoprecipitation assay buffer (Beyotime, China) with additional mixture inhibitor (Roche), sonicated for 15 s, and centrifuged at 14,000 × g for 8 min at 4 °C. Proteins resolved by PAGE in 15% SDS were transferred onto polyvinylidene fluoride membranes (Millipore), which were incubated with specific primary antibodies at 4 °C overnight, followed by incubation with secondary antibodies for no less than 2 h. Visualization was then performed with the enhanced chemiluminescence plus detection system (PerkinElmer) and Kodak film.

Real-Time PCR. Total RNA was prepared by using the RNA Extract Kit (Tiangen). First-Strand complementary DNA (cDNA) was synthesized by M-MLV reverse enzyme (Takara). With specific primers and SYBR Green qPCR master mix, RT-PCR reactions were performed under the following protocol: initial denaturation at 95 °C for 3 min, followed by 40 cycles of three steps each at 95 °C for 30 s, 60 °C for 30 s, and 72 °C for 30 s. Relative expression levels of different genes were normalized to that of GAPDH (26). Primers used are listed in Dataset S2.

MicroRNA (miRNA) Assays. Small RNA was extracted from cell lysates with miRNeasy (Qiagen) and analyzed by following the instructions of the All-in-One miRNA qPCR Detection Kit (GeneCopoeia), with universal reverse primer and specific forward primer.

Bliss Independent Criterion Analysis. This analysis was performed as reported previously (27, 28). Inhibition by tamoxifen (TAM), AZD1480, and the combination was measured by using the 3-(4,5-dimethyl-2-thiazolyl)-2,5-diphenyl -2-H-tetrazolium bromide (MTT) assay. The theoretical inhibition rate was calculated as E (Bliss) = E (TAM) + E (AZD) − E (TAM) × E (AZD). If the observed inhibition rate E (observed) is more than the theoretical inhibition rate, E (Bliss), the two drugs are considered to have synergetic effects.

Xenograft Studies. All in vivo experiments were conducted in an SPF (specific pathogen-free) laboratory. Six-week-old NOD-SCID mice were purchased from Vital River. MCF7-shCtrl or MCF7-shZIP cells were suspended in serum-free Dulbecco's modified Eagle's medium, and 10^6 cells were injected in the

mammary fat pads and allowed to grow for 6 wk. After 3 d, tumor-bearing mice were treated by intragastric introduction with vehicle or tamoxifen dissolved into PBS, 25 mg/kg/d every 3 d (29). The volume was calculated as $(4\pi/3)$ $(\text{width}/2)^2$ $(\text{length}/2)$. The tumor weight was measured at the ending point. The procedures were performed according to the *Laboratory Animals—Guideline of Welfare and Ethics* (30) of the Standardization Administration of the People's Republic of China and regulations of local ethical approval; $n = 6$ for each group.

Statistical Analysis. Experiments were performed in triplicate. Column heights indicate mean values. Bars indicate SDs. Comparisons between two groups were performed using paired one-tailed *t* tests. Results are reported as mean + SD unless otherwise noted. All in vitro experiments were performed three times at least. $*P < 0.05$, $**P < 0.01$, $***P < 0.001$. NS indicates not significant.

Patient Specimens. The tamoxifen-treated specimens were from six female patients. They were first diagnosed as bearing ER+ breast cancer and chose to undergo tamoxifen-adjuvant chemotherapy, together with 5-FU, THP-adriamycin, or cyclophosphamide, instead of a mastectomy. During the course of treatment, ranging from 3 mo to 5 y, they experienced recurrent cancers and then accepted a mastectomy. The non-tamoxifen-treated breast cancer control patients underwent chemotherapy with 5-FU, THP-adriamycin, and cyclophosphamide, etc., but not tamoxifen. They also experienced recurrent cancers and accepted a mastectomy.

Proteins from cancerous tissue as well as normal tissue (located at least 3 cm away from cancerous tissue) were extracted to perform Western analysis. The patient specimens were generated by the Gansu Provincial Cancer Hospital (GPCH) in compliance with protocols approved by the GPCH Institutional Review Board after the subjects gave their consent.

Results

Identification of dZIP in Tamoxifen-Resistant MCF7 Cells. Lentiviruses encoding the three VBIM viruses were used to drive random mutations in populations of ER-positive MCF7 breast tumor cells. Following selection with Tamoxifen, we transfected a vector encoding CRE recombinase into resistant colonies (Fig. 1*A* and *SI Appendix*, Fig. S1*A*), finding that four of eight colonies showed dependence on the CMV promoter for resistance. In validated colony R2, a DNA fragment flanking the SD2 insertion site was mapped to the ZIP gene, on chromosome 20q13 (Fig. 1*B*), a hot spot locus that includes many genes related to tamoxifen resistance (31). This insertion led to the expression of a truncated ZIP protein (dZIP) with 329 amino acids instead of full-length ZIP, which has 511 (Fig. 1 *C* and *D*). The mutant of this gene was detected once in our screening. dZIP lacks the C3H1 zinc finger DNA binding domain. The NuRD complex is a key regulator of histone deacetylation and repression of transcription (32, 33), and ZIP has been reported to associate with components of this complex (18). NuRD mediates histone deacetylation and target gene silencing. As reported, the loss of the zinc finger domain of ZIP leads to a mutant protein in which the ability to bind the NuRD complex is unimpaired but the ability to recognize specific promoters is lost, resulting in a dominant-negative function (19, 34). When overexpressed in naive MCF7 cells, dZIP conferred resistance to tamoxifen (Fig. 1*E* and *SI Appendix*, Fig. S1*B*).

ZIP Expression Reverses Tamoxifen Resistance in Breast Cancers. To study the role of full-length ZIP in tamoxifen resistance in breast cancer cells more broadly, we investigated the sensitivity to tamoxifen in different ERα-positive breast cancer cell lines. ZR-75-30 (ZR) is relatively resistant to tamoxifen treatment, while MCF7 and T47D are sensitive (*SI Appendix*, Fig. S2*A*). To study whether endogenous ZIP contributes to tamoxifen sensitivity in responsive cells, we repressed its expression in MCF7 and T47D cells with small hairpin RNAs (shRNAs) (Fig. 2*A* and *SI Appendix*, Fig. S2*B*). Down-regulation of ZIP elevated tamoxifen resistance in both cell lines (Fig. 2*A* and *SI Appendix*, Fig. S2*B*). ZR-ZIP cells, which have increased expression of ZIP, are more sensitive than control cells (Fig. 2*B*). These results indicate that tamoxifen resistance can be reversed by increased ZIP expression and that endogenous ZIP is a regulator of tamoxifen sensitivity in vitro.

In contrast to estrogen, after it binds to the ER, tamoxifen recruits different proteins as corepressors, such as NCoR (nuclear receptor corepressor) and SMRT, which repress gene stimulation. Therefore, we evaluated the effect of fulvestrant, an inhibitor of ER signaling that is not dependent on association with corepressors. We found that knockdown of ZIP in MCF7 and T47D cells increased resistance to fulvestrant, while overexpression of ZIP had no effect on ZR cells treated with the chemical. This result correlated with the dependence on the estrogen receptor (*SI Appendix*, Fig. S2*C*), indicating that ZIP may affect ER expression and/or activation.

To confirm the in vivo role of ZIP in regulating resistance, responses to tamoxifen were tested in immunodeficient mouse models bearing MCF7-shControl (shC) or MCF7-shZIP (sh2) xenografts. Obvious differential inhibition of tumor growth between experimental and control groups was observed (Fig. 2*C* and *SI Appendix*, Fig. S2 *D* and *E*), indicating the tumor-repressing effect of tamoxifen. The growth of control shC

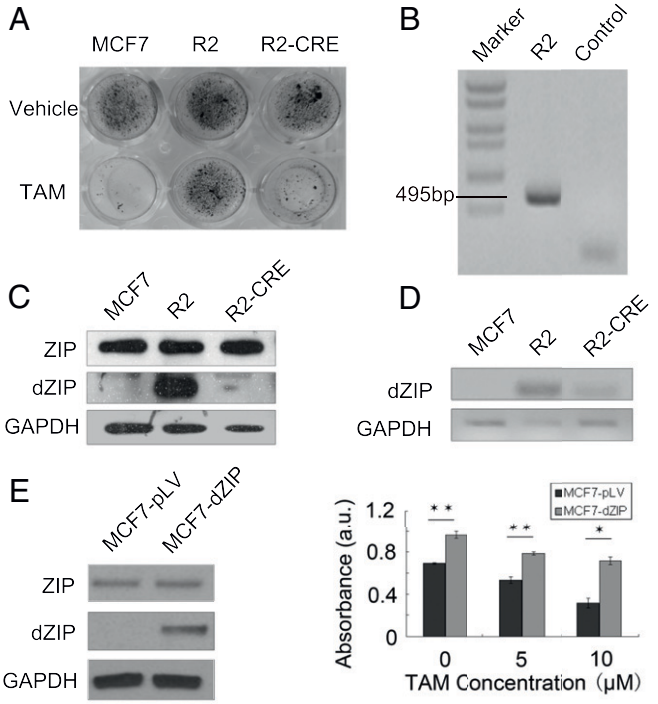

Fig. 1. Forward genetics identifies dZIP, a truncated form of ZIP, in tamoxifen-resistant R2 cells. (*A*) A population of MCF7 cells was infected with the VBIM lentiviruses and selected with tamoxifen. R2 was a VBIM-positive single colony resistant to TAM. R2 was transfected with a vector encoding CRE recombinase to generate R2-CRE cells and then treated again with tamoxifen. Surviving cells were stained with crystal violet. (*B*) Genomic DNAs from control MCF7 cells or R2 cells were digested and self-ligated. Nested PCR was performed to obtain the sequence flanking the insertion. (*C*) Western analysis was performed to measure the expression of ZIP and dZIP in MCF7, R2, and R2-CRE cells. GAPDH served as the loading control. (*D*) The expression of dZIP mRNA was analyzed by RT-PCR using a 5′ primer for FLAG sequences and a 3′ primer for ZIP. GAPDH served as the loading control. (*E*) Ectopic expression of dZIP in naive MCF7 cells leads to tamoxifen resistance. (*Left*) MCF7 cells were infected with a lentivirus encoding dZIP, and total lysates were analyzed by the Western method. (*Right*) The absorbance at 570 nm of the diluted crystal violet was measured and analyzed in three independent experiments. $*P < 0.05$, $**P < 0.01$.

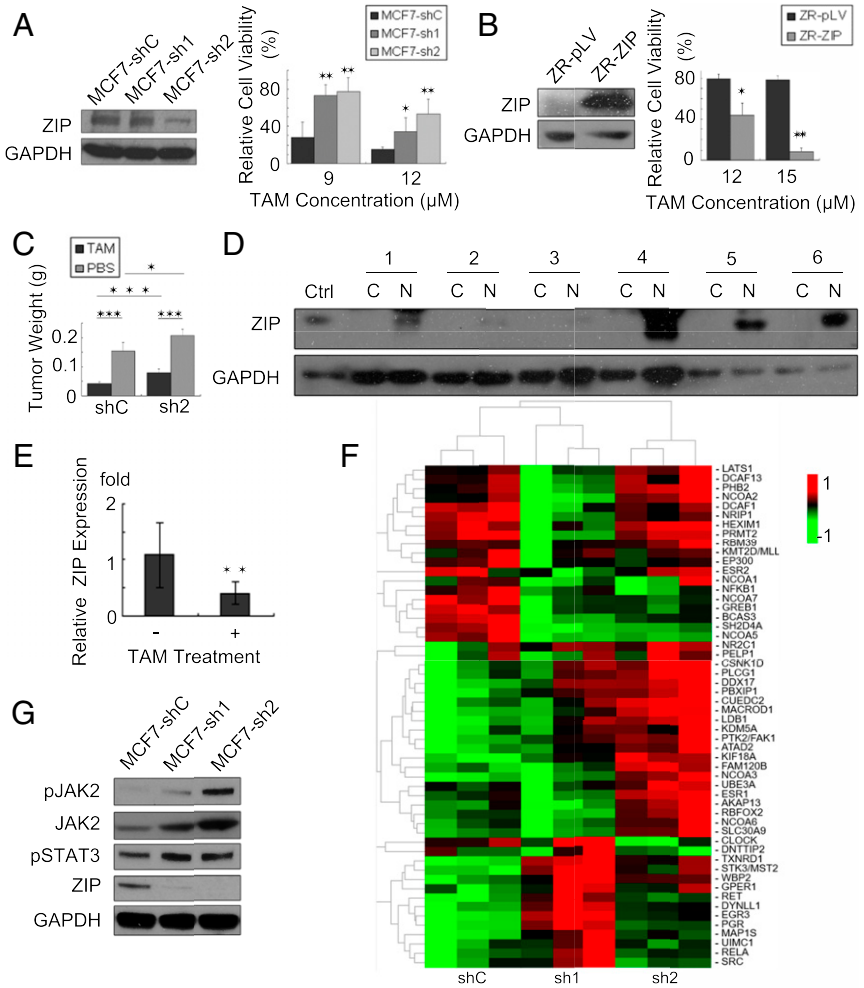

Fig. 2. ZIP is a negative regulator of tamoxifen resistance. (*A*, *Left*) MCF7 cells were infected with lentiviruses encoding shRNAs targeting ZIP, and total protein lysates were analyzed by the Western method. (*A*, *Right*) TAM was added, and cell viability was evaluated using the MTT assay ($n = 4$). (*B*) ZR-75-30 (ZR) cells were infected with a lentivirus encoding full-length ZIP. Protein expression (*Left*) and relative cell viability (*Right*) were analyzed as in *A*. $n = 4$. (*C*) In vivo efficacy of tamoxifen on breast tumor xenografts expressing different levels of ZIP. Weights of tumors from mice bearing MCF7-shC control or MCF7-shZIP (sh2) xenografts, with or without TAM treatment, were determined ($n = 6$). (*D*) ZIP expression in human breast cancer patients. Tumor samples were assayed by the Western method. A lysate from MDA-MB-468-ZIP cells was used as a positive control. C: cancerous tissue; N: normal tissue. (*E*) Relative expression of ZIP in *SI Appendix*, Fig. S1*F* was analyzed. The mean fold changes of ZIP mRNA expression in 21 patients who were not treated with TAM and 6 patients who were treated with TAM were analyzed with unpaired two-tailed Student's *t* tests. (*F*) Relative mRNA expression change of ER-related genes in MCF7-shControl (shC) vs. shZIP (sh1 and sh2). Hierarchical heat map displaying expression values for ER cofactors or related genes. Read numbers from RNA-seq data were normalized with minimum–maximum scaling. Red shows up-regulation, and green shows down-regulation. Three replicates from each cell line are shown. (*G*) MCF7 or T47D cells were infected with lentiviruses encoding shRNAs targeting different sites of ZIP, and total lysates and protein samples were analyzed by the Western method. $^*P < 0.05$, $^{**}P < 0.01$, $^{***}P < 0.001$.

xenografts was greatly impaired compared to sh2 xenografts upon treatment with tamoxifen.

We also compared each normal mammary gland tissue with the corresponding recurrent/resistant cancer specimen (described in *Materials and Methods*), observing dramatic down-regulation of ZIP expression in all six tamoxifen-treated tumor samples (Fig. 2*D*). Comparing the relative expression of ZIP in samples from tamoxifen-treated vs. untreated breast tumor patients, we also observed significant down-regulation in the tamoxifen-treated samples (Fig. 2*E* and *SI Appendix*, Fig. S2*F*).

ZIP Regulates Tamoxifen Sensitivity by Affecting Multiple Pathways. To further address how the expression of ZIP changes the sensitivity to tamoxifen, we examined ERα, the target of tamoxifen, and genes that are directly regulated by ERα (*SI Appendix*, Fig. S3*B*). ERα expression was elevated in exogenous ZIP-expressing cells and down-regulated in ZIP-knockdown cells (*SI Appendix*, Fig. S3*B*). We also found down-regulation of ERα-dependent genes, such as *CATHD, MYC, EGR3, GREB1,* and *RET* (*SI Appendix*, Fig. S3*C*). These results strongly indicated that ZIP suppresses expression of ERα along with its target genes. To discover whether additional genes related to the ER pathway or other important signaling pathways were also regulated by ZIP knockdown, we performed an RNA sequencing analysis in MCF7-shC cells, compared to MCF7-shZIP cells, finding that many ER cofactors and downstream genes were affected, either directly or indirectly (Fig. 2*F*). Since ZIP has a zinc finger domain that is required for DNA binding and loss of this domain enhances resistance to tamoxifen, we performed ChIP sequencing assays in MCF7 cells stably expressing FLAG-tagged ZIP to reveal key drivers of tamoxifen resistance, finding that the protein products of ZIP target genes function in several important

pathways, including regulation of signal transduction, giving us additional clues concerning possible mechanisms of resistance (*SI Appendix*, Fig. S3*A*).

After long-term exposure of SERMs (selective estrogen receptor modulators) in breast cancer cells, many pathways have been reported to regulate tamoxifen sensitivity. Breast cancer anti-estrogen resistance 1, 2, and 3 (BCAR1, 2 and 3) and RTKs modulate tamoxifen resistance either by stimulating the expression or activation of proliferation factors or by suppressing cell death genes (35, 36). We found that the expression of all three BCARs was not elevated but reduced, indicating that these proteins are not essential to mediate tamoxifen resistance induced by ZIP knockdown (*SI Appendix*, Fig. S3*D*). RTKs, including EGFR, HER2, PDGFR, and IGF1R, play important roles in endocrine chemotherapy resistance by regulating the activities of genes whose products can bypass the function of ERα in breast cancer (6). In cells lacking ZIP, the expression of EGFR and HER2, but not of IGF1R or PDGFR, was up-regulated (*SI Appendix*, Fig. S3*E*). We found that the activation level of EGFR, but not HER2, was elevated in ZIP-knockdown cells (Fig. 2*G* and *SI Appendix*, Fig. S3*E*) and that EGFR was one of the mediators through which ZIP regulated ERα expression (*SI Appendix*, Fig. S3*H*). This result is in agreement with the previous finding that ZIP represses EGFR and suppresses breast carcinogenesis. In these cells, we also found expression of p21-activated kinase 1 was suppressed, which has been reported to predict tamoxifen failure in primary tumors (*SI Appendix*, Fig. S3*G*). We also found that most of the miRNAs that regulate TAM sensitivity, including mir101, mir206, and mir221/mir222, were not dramatically suppressed by ZIP knockdown (*SI Appendix*, Fig. S3*I*). Therefore, we conclude that ZIP does not suppress the expression and activity of BCARs and most of RTKs, which suggests that the loss of ZIP-induced tamoxifen resistance is not through induction of these classical chemoresistance genes.

In addition to the pathways noted above, we also investigated the activity of other potential ZIP downstream pathways, including MAPK-ERK, PI3K-PTEN/AKT/mTOR, PKA and PAK1, NFκB, etc. Phosphorylation of IKKα/β was elevated, while pIκB was repressed, in T47D cells (*SI Appendix*, Fig. S3*E*). In TNBC cells, BT549 and MDA-MB-231, PTEN, and EGFR were repressed when ZIP was overexpressed (*SI Appendix*, Fig. S3*J* and ref. 35). Then we tested the combination of TAM with the inhibitors against these regulated factors. We found that pathways of EGFR, AKT/mTOR, and NFκB, but not HER2, were involved in (*SI Appendix*, Fig. S3*K*).

ZIP Represses STAT3 Activation by Regulating JAK2 Expression. As a critical transcription factor, STAT3 plays important roles in cancer progression and chemoresistance (10). We asked whether STAT3 is involved in the regulation of tamoxifen sensitivity by ZIP. The level of activated STAT3 was elevated in shZIP cells (Fig. 2*G*). Furthermore, knockdown of STAT3 in ZIP-knockdown cells reduced the resistance caused by ZIP inactivation (*SI Appendix*, Fig. S4*A*). Therefore, ZIP modulates tamoxifen sensitivity, at least partly, by regulating STAT3 activation in breast cancer cells.

Since EGFR was reported to directly activate STATs (28, 37), we also investigated whether EGFR activates STAT3 in ZIP-knockdown cells, finding that knockdown of EGFR did not affect the tyrosine phosphorylation of STAT3 in these cells (*SI Appendix*, Fig. S4*A*). Among potential ZIP target genes discovered by ChIP-seq, JAK2 is an important regulator of STAT activation and is also involved in responses to growth factors (38, 39). Interestingly, in MCF7-shZIP cells, respective treatment with the JAK inhibitor AZD1480 (40) efficiently suppressed the phosphorylation of STAT3 but had minimal effects on cell viability (*SI Appendix*, Fig. S4*B*), indicating that JAK2 may participate in STAT3 activation that is driven by ZIP. Furthermore, the Bliss independent criterion (*Materials and Methods*) showed that combining AZD1480, a JAK inhibitor, with tamoxifen enhanced the inhibitory effect of tamoxifen (Fig. 3*A*).

In addition, overexpression of ZIP in ZR cells that are tamoxifen resistant and express low levels of ZIP efficiently suppressed JAK2 expression, as well as JAK2 and STAT3 activation (Fig. 3*B* and *SI Appendix*, Fig. S4*C*). A JAK2-specific shRNA also inactivated STAT3 phosphorylation, up-regulated ERα expression level, and increased tamoxifen sensitivity (Fig. 3*C* and *SI Appendix*, Fig. S4 *D–H*). Interestingly, ectopic expression of ZIP in 231 or BT549 cells also decreased JAK2 expression and the levels of phosphorylated STAT3 (*SI Appendix*, Fig. S4 *I* and *J*).

Ruxolitinib, a potent inhibitor of JAKs 1 and 2, has been approved for the treatment of myelofibrosis. To explore the potential effect of combining two approved drugs, we treated MCF7shZIP cells with tamoxifen and ruxolitinib together. This combination strongly enhanced the inhibitory effect seen with tamoxifen alone (*SI Appendix*, Fig. S4*K*), but ruxolitinib alone had no substantial effect on cell viability, although it did inhibit JAK2 activity (*SI Appendix*, Fig. S4*L*). We conclude that a JAK or STAT3 inhibitor might be a useful addition to tamoxifen in treating a specific group of breast cancer patients (41).

If JAK2 is the most important effector downstream of ZIP and upstream of STAT3, in JAK2 wild-type (WT) cells, we expect that ZIP would suppress STAT3 activation, while in JAK2-null cells, ZIP would not. γ2a is a JAK2-knockout cell line derived from 2fTGH cells. As expected, ZIP overexpression suppressed the phosphorylation of STAT3 in parental 2FTGH, TYK2-deficient U1A mutant cells, and JAK1-deficient U4A mutant cells, but not in γ2A cells (Fig. 3*D*).

Moreover, in the Cancer Genome Atlas (TCGA) data from total breast cancer cases (n = 1,100), there is a −0.33 correlation value between ZIP and JAK2, supporting the conclusion that the expression of those two factors is negatively correlated (Fig. 3*E*). Especially, this negative correlation is statistically significant in normal, luminal A, and luminal B subtypes (Fig. 3*F*).

In summary, the expression of ZIP was repressed in tamoxifen-resistant breast cancer specimens compared to paired control normal tissues. And in vitro, the levels of ZIP expression are inversely correlated with the levels of JAK2 and phosphorylated STAT3. These data confirm that ZIP regulates STAT3 activity by regulating JAK2 expression. Increased expression of JAK2 in MCF7 cells failed to activate STAT3 or induce tamoxifen resistance (*SI Appendix*, Fig. S4*M*), indicating that JAK2 activation is also required. A genome-wide RNA-seq analysis of MCF7-shC and -shZIP cells helped us to find additional ZIP-regulated genes that are involved in the JAK-STAT pathway (*SI Appendix*, Fig. S5 and Dataset S4).

ZIP Regulates JAK2 Expression by Directly Binding to Its Promoter. To address whether ZIP regulates JAK2 expression directly, we searched DNA sequences in and near the JAK genes, finding potential ZIP binding sites upstream of *JAK2* (Fig. 4*A*). The element GGAGg/aAg/aA was based on an analysis from a cyclic amplification and selection of target assay (18), in which immobilized ZIP protein binds to specific DNA sequences, with the finding that 80 of 93 sequences contained a GA-rich element. To test whether ZIP binds to the *JAK2* gene, we performed a ChIP assay in 293T cells transfected with the pCDNA3.1-FLAG-ZIP plasmid. ZIP-FLAG immunoprecipitated DNA fragments flanking both the GGAGAAGA sequence at −6226 to −6219 bp and the sequence at −5482 to −5475 bp (upstream from the ATG start codon) but not fragments from similar sites upstream or downstream, flanking −8745 to −8738 or −155 to −148 bp (Fig. 4*B*). Interestingly, we also found that ZIP can bind to the upstream region of its own gene, at −2132 GGAGGAAA −2125 (upstream from the ATG start codon) (Fig. 4*B*).

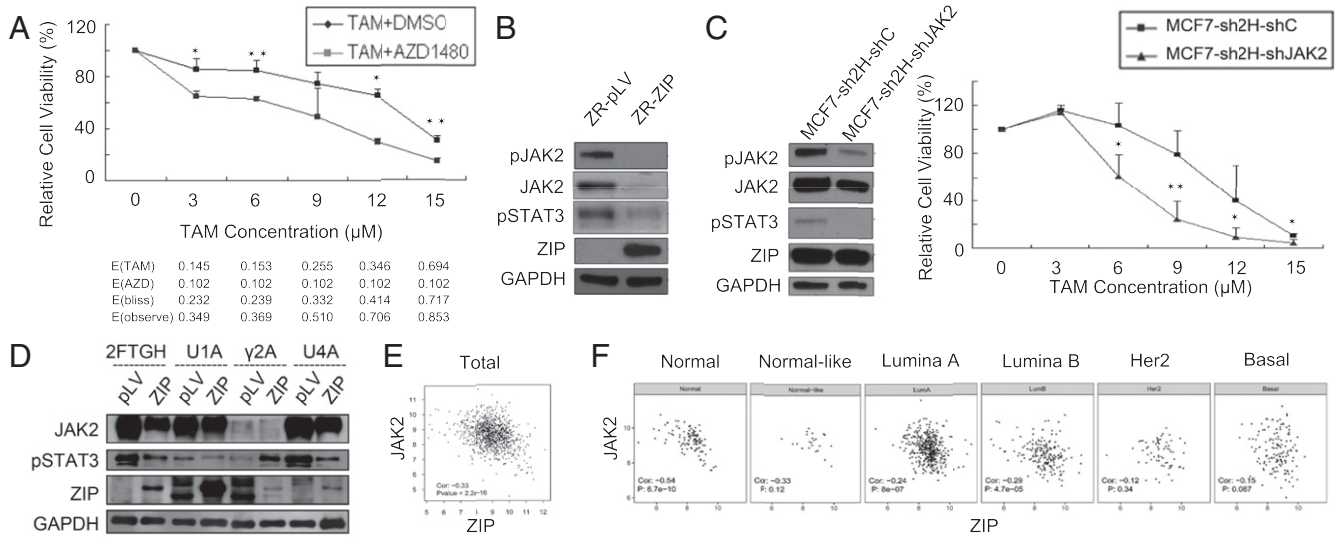

Fig. 3. The ability of ZIP to reverse resistance to tamoxifen is partly induced by the phosphorylation of STAT3. (*A*) A JAK2 inhibitor enhances the effect of TAM. Cells were treated with tamoxifen alone or together with AZD1480, and MTT assays were performed. $n = 3$. (*B*) ZIP overexpression down-regulates STAT3 and JAK2 phosphorylation. Total proteins from control or ZIP-overexpressed ZR cells were assayed by the Western method for phosphorylated JAK2, total JAK2, phosphorylated STAT3, and total STAT3. (*C*, *Left*) Total proteins from JAK2-knockdown or control MCF7-shZIP cells were analyzed by the Western method for phosphorylated JAK2, total JAK2, phosphorylated STAT3, or total STAT3. (*C*, *Right*) MTT assays were performed to test viability following treatment with tamoxifen. (*D*) TYK2-deficient U1A mutant cells, JAK1-deficient U4A mutant cells, JAK2-deficient γ2A mutant cells, and parental 2fTGH (WT) cells were infected with a control lentivirus or a virus encoding ZIP. Total lysates were analyzed for total JAK2, phosphorylated STAT3, and ZIP. GAPDH was used as the loading control. (*E* and *F*) ZIP expression was negatively correlated with JAK2. Expression levels of ZIP and JAK2 in TCGA total breast cancer cases ($n = 1{,}100$), as well as subtype-specific breast cases from RNA-seq data, are plotted. $^*P < 0.05$, $^{**}P < 0.01$.

To investigate whether ZIP regulates *JAK2* transcription, we cloned fragments of the *JAK2* upstream regulatory region into luciferase reporter vectors, made mutations in both binding elements, and stably transfected these vectors into 293T cells. Then we transiently transfected ZIP or control expression vectors into these cells (Fig. 4*C*). Mutation of the ZIP binding site in the *JAK2* upstream sequence obviously hindered the ability of ZIP to repress expression in a dose-dependent manner (Fig. 4*D*). Our data indicate that ZIP represses JAK2 expression directly and thus down-regulates STAT3 activation. Although JAK2 expression is

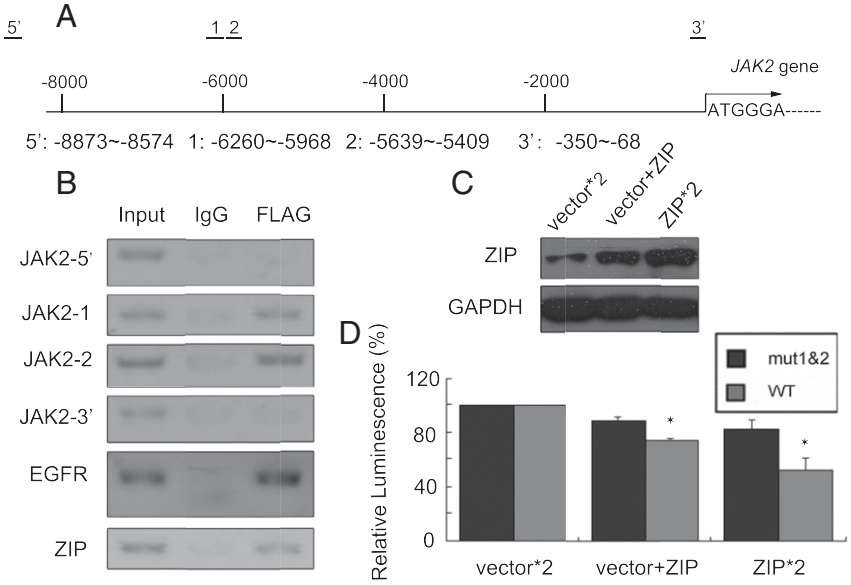

Fig. 4. ZIP binds to the JAK2 promoter and regulates gene expression. (*A*) ZIP target sequences in the JAK2 locus. Sequence lengths and locations relative to the ATG start codon are shown. (*B*) The JAK2 promotor is targeted by ZIP. ChIP assays were performed to confirm the occupation of potential target sequences. (*C*) Transient overexpression of ZIP in 293T cells. The expression level of ZIP was assayed by the Western method. (*D*) ZIP represses JAK2 promotor-driven luminescence. The 293T cells were stably transfected with luciferase vectors driven by the mutation GGAggAGA to GGActAGA, or wild-type JAK2 promoters. Vectors encoding ZIP or controls were transfected into the cells, and luminescence was measured 24 h later. Values were normalized to cells infected with only control vectors. Each bar represents the mean of triplicate experiments. $^*P < 0.05$.

necessary to mediate tamoxifen resistance, activation of JAK2 by one or more cytokines is also required (42).

Discussion

The ZIP gene is located at 20q13, a hot spot that includes additional genes related to tamoxifen resistance (31). The ZIP protein represses the expression of its target genes by binding to specific sequences in their promoters, followed by recruitment of the NuRD complex to establish a condensed chromatin state by a universal deacetylation mechanism (18). We found that suppression of ZIP expression resulted in regulation of multiple pathways, especially suppression and inactivation of ERα (*SI Appendix*, Fig. S3 *A*–*C*).

ChIP-seq data indicated that JAK2 might be a regulator of STAT activity in response to ZIP. We searched for DNA sequences in and near the JAK genes, finding potential ZIP binding sites upstream of *JAK2* (Fig. 4*A*). Consistently, overexpressing ZIP suppressed the expression of JAK2 mRNA and protein (Fig. 3*B* and *SI Appendix*, Fig. S4 *C*, *I*, and *J*). There is also a ZIP target sequence −2132 to −2125 bp upstream of the coding region of the *ZIP* gene itself that could be recognized by the ZIP protein (Fig. 4*B*), suggesting that ZIP inhibits its own expression, establishing a negative feedback loop. By that means, it may be possible to balance histone acetylation and gene expression more readily (19).

As a consequence of the decrease in JAK2 expression, phosphorylated STAT3 was also down-regulated by ZIP (Fig. 3*B* and *SI Appendix*, Fig. S4 *I* and *J*). Although knockdown of JAK2 expression resulted in STAT3 inactivation and tamoxifen sensitization, overexpression of JAK2 in MCF7 cells did not lead to STAT3 phosphorylation or tamoxifen resistance (*SI Appendix*, Fig. S4*M*), indicating that the level of JAK2 expression is not itself sufficient to drive STAT3 activation, almost certainly because activation of JAK2 by appropriate cytokines is also required (Dataset S4). In addition, the expression of many genes directly targeted by ZIP, including several genes involved in tumor progression (43, 44), was up-regulated rather than suppressed, implying additional mechanisms of the ZIP function.

The V617F mutation of JAK2 is found in about 95% of patients with polycythemia vera and about 50% of patients with essential thrombocythemia or primary myelofibrosis (45). This mutation is one of the most common abnormalities in myeloproliferative neoplasms (36), highlighting mutated JAK2 as a therapeutic target in several diseases (46). However, clinical trials of JAK2 V617F inhibitors reveal that targeting this protein might be difficult (47, 48). Thus, negative regulators such as ZIP can suppress the expression of both JAK2 and JAK2V617F and may provide another approach to modulate the expression of this mutated protein. Because there is significant overlap in signaling, cells simultaneously employ multiple pathways to activate proliferation, survival, angiogenesis, metastasis, and drug resistance. This flexibility enables tumors to bypass the stress of treatment with a single drug, revealing the necessity of combining therapeutic modalities. Our data revealing that AZD1480 enhances the inhibitory effect of tamoxifen provide a rationale for combining hormone therapy with inhibition of JAK-STAT signaling (Fig. 3*A*). Ruxolitinib (INCB018424), a selective inhibitor of both JAK1 and JAK2, is an orally available drug that has been evaluated extensively in clinical trials. It is the first FDA-approved JAK2 inhibitor for treating myelofibrosis (49). Our data concerning the expression and activation status of JAK2 and STAT3 support the possibility that ruxolitinib, in combination with tamoxifen, may benefit a specific subset of breast cancer patients (*SI Appendix*, Fig. S4 *K* and *L*).

STAT3 is an important therapeutic target in several kinds of cancers (50, 51) since the effectiveness of therapy is hindered when STAT3 is activated. There is currently some information concerning specific molecular mechanisms that govern drug resistance in response to STAT3 activation. MDR1, a STAT3-responsive gene important in resistance (52), encodes a protein in the ABC family that pumps many different drugs out of cells, thus reducing their intracellular levels. Several other proteins, including MRP1 and TOPOII, which are regulated coordinately with STAT3, are also therapeutic targets (53).

Our data also indicate that ZIP may serve as a prognostic biomarker (Fig. 2*D*). We surveyed an online database to assess the relevance of the levels of expression of different mRNAs on clinical outcomes for breast tumor patients (54). Interestingly, higher ZIP expression predicts a better prognostic outcome (hazard ratio = 0.7, CI = 0.54 to 0.91, $P = 0.0076$) in the group of 1,045 ERα-positive patients in which TAM was used as adjuvant treatment, supporting the idea that ZIP expression can be used as a biomarker for predicting prognosis and responses to selective estrogen receptor modulators, such as tamoxifen (*SI Appendix*, Fig. S6).

ACKNOWLEDGMENTS. This work was funded by NIH Grant PO1 CA062220 (to G.R.S.) and by Major Science and Technology Innovation Project for Marine Drugs of Shandong Province Grant 2018SDKJ0402-3, National Science and Technology Major Project for Significant New Drugs Development Grant 2018ZX09735-004, and National Natural Science Foundation of China Grant 31571439 (to J.Y.). We thank Dr. Yongfeng Shang and Dr. Sapin Constantinescu for generously sharing plasmids and Dr. Xuan Liu for helpful technical support and discussions. We thank Hongyun Guo for assistance with patient samples from The Bank of Patient Specimens, Gansu Provincial Cancer Hospital, Gansu Provincial Academic Institute for Medical Research.

1. J. C. Keen, N. E. Davidson, The biology of breast carcinoma. *Cancer* **97** (suppl. 3), 825–833 (2003).
2. B. J. Deroo, K. S. Korach, Estrogen receptors and human disease. *J. Clin. Invest.* **116**, 561–570 (2006).
3. C. K. Osborne, Tamoxifen in the treatment of breast cancer. *N. Engl. J. Med.* **339**, 1609–1618 (1998).
4. Anonymous, Tamoxifen for early breast cancer: An overview of the randomised trials. Early breast cancer trialists' collaborative group. *Lancet* **351**, 1451–1467 (1998).
5. R. I. Nicholson *et al.*, Epidermal growth factor receptor expression in breast cancer: Association with response to endocrine therapy. *Breast Cancer Res. Treat.* **29**, 117–125 (1994).
6. R. B. Riggins, R. S. Schrecengost, M. S. Guerrero, A. H. Bouton, Pathways to tamoxifen resistance. *Cancer Lett.* **256**, 1–24 (2007).
7. Y. Wu *et al.*, Tamoxifen resistance in breast cancer is regulated by the EZH2-ERα-GREB1 transcriptional axis. *Cancer Res.* **78**, 671–684 (2018).
8. R. I. Nicholson, J. M. Gee, Oestrogen and growth factor cross-talk and endocrine insensitivity and acquired resistance in breast cancer. *Br. J. Cancer* **82**, 501–513 (2000).
9. J. E. Darnell Jr., I. M. Kerr, G. R. Stark, Jak-STAT pathways and transcriptional activation in response to IFNs and other extracellular signaling proteins. *Science* **264**, 1415–1421 (1994).
10. E. B. Haura, J. Turkson, R. Jove, Mechanisms of disease: Insights into the emerging role of signal transducers and activators of transcription in cancer. *Nat. Clin. Pract. Oncol.* **2**, 315–324 (2005).
11. R. Buettner, L. B. Mora, R. Jove, Activated STAT signaling in human tumors provides novel molecular targets for therapeutic intervention. *Clin. Cancer Res.* **8**, 945–954 (2002).
12. J. Yang *et al.*, Unphosphorylated STAT3 accumulates in response to IL-6 and activates transcription by binding to NFkappaB. *Genes Dev.* **21**, 1396–1408 (2007).
13. J. Yang *et al.*, Reversible methylation of promoter-bound STAT3 by histone-modifying enzymes. *Proc. Natl. Acad. Sci. U.S.A.* **107**, 21499–21504 (2010).
14. H. Lee *et al.*, Acetylated STAT3 is crucial for methylation of tumor-suppressor gene promoters and inhibition by resveratrol results in demethylation. *Proc. Natl. Acad. Sci. U.S.A.* **109**, 7765–7769 (2012).
15. L. Li, P. E. Shaw, Autocrine-mediated activation of STAT3 correlates with cell proliferation in breast carcinoma lines. *J. Biol. Chem.* **277**, 17397–17405 (2002).
16. X. Chen *et al.*, Brevilin A, a novel natural product, inhibits janus kinase activity and blocks STAT3 signaling in cancer cells. *PLoS One* **8**, e63697 (2013).
17. J. Zhang *et al.*, Dehydrocrenatidine is a novel janus kinase inhibitor. *Mol. Pharmacol.* **87**, 572–581 (2015).
18. R. Li *et al.*, ZIP: A novel transcription repressor, represses EGFR oncogene and suppresses breast carcinogenesis. *EMBO J.* **28**, 2763–2776 (2009).
19. B. Gui *et al.*, Dimerization of ZIP promotes its transcriptional repressive function and biological activity. *Int. J. Biochem. Cell Biol.* **44**, 886–895 (2012).
20. T. Lu *et al.*, Validation-based insertional mutagenesis identifies lysine demethylase FBXL11 as a negative regulator of NFkappaB. *Proc. Natl. Acad. Sci. U.S.A.* **106**, 16339–16344 (2009).

21. C. Guo, G. R. Stark, FER tyrosine kinase (FER) overexpression mediates resistance to quinacrine through EGF-dependent activation of NF-kappaB. *Proc. Natl. Acad. Sci. U.S.A.* **108**, 7968–7973 (2011).
22. R. Cipriano *et al*., FAM83B mediates EGFR- and RAS-driven oncogenic transformation. *J. Clin. Invest.* **122**, 3197–3210 (2012).
23. W. Jiang *et al*., Forward genetic screening for regulators involved in cholesterol synthesis using validation-based insertional mutagenesis. *PLoS One* **9**, e112632 (2014).
24. S. De, R. Cipriano, M. W. Jackson, G. R. Stark, Overexpression of kinesins mediates docetaxel resistance in breast cancer cells. *Cancer Res.* **69**, 8035–8042 (2009).
25. D. Watling *et al*., Complementation by the protein tyrosine kinase JAK2 of a mutant cell line defective in the interferon-gamma signal transduction pathway. *Nature* **366**, 166–170 (1993).
26. J. He *et al*., STAT3 mutations correlated with hyper-IgE syndrome lead to blockage of IL-6/STAT3 signalling pathway. *J. Biosci.* **37**, 243–257 (2012).
27. M. Goldoni, C. Johansson, A mathematical approach to study combined effects of toxicants in vitro: Evaluation of the Bliss independence criterion and the Loewe additivity model. *Toxicol. In Vitro* **21**, 759–769 (2007).
28. J. Nan *et al*., TPCA-1 is a direct dual inhibitor of STAT3 and NF-κB and regresses mutant EGFR-associated human non-small cell lung cancers. *Mol. Cancer Ther.* **13**, 617–629 (2014).
29. A. Deronic, S. Tahvili, T. Leanderson, F. Ivars, The anti-tumor effect of the quinoline-3-carboxamide tasquinimod: Blockade of recruitment of CD11b(+) Ly6C(hi) cells to tumor tissue reduces tumor growth. *BMC Cancer* **16**, 440 (2016).
30. Standardization Administration of the People's Republic of China, Laboratory animals—Guideline of welfare and ethics (2016). https://wenku.baidu.com/view/b6803f99951ea76e58fafab069dc5022aaea468b.html. Accessed 23 May 2020.
31. P. Y. Hsu *et al*., Amplification of distant estrogen response elements deregulates target genes associated with tamoxifen resistance in breast cancer. *Cancer Cell* **24**, 197–212 (2013).
32. O. Yildirim *et al*., Mbd3/NURD complex regulates expression of 5-hydroxymethylcytosine marked genes in embryonic stem cells. *Cell* **147**, 1498–1510 (2011).
33. C. Aguilera *et al*., c-Jun N-terminal phosphorylation antagonises recruitment of the Mbd3/NuRD repressor complex. *Nature* **469**, 231–235 (2011).
34. W. Yu, R. Li, B. Gui, Y. Shang, sZIP, an alternative splice variant of ZIP, antagonizes transcription repression and growth inhibition by ZIP. *J. Biol. Chem.* **285**, 14301–14307 (2010).
35. A. Brinkman, S. van der Flier, E. M. Kok, L. C. Dorssers, BCAR1, a human homologue of the adapter protein p130Cas, and antiestrogen resistance in breast cancer cells. *J. Natl. Cancer Inst.* **92**, 112–120 (2000).
36. T. van Agthoven *et al*., Identification of BCAR3 by a random search for genes involved in antiestrogen resistance of human breast cancer cells. *EMBO J.* **17**, 2799–2808 (1998).
37. M. Colomiere *et al*., Cross talk of signals between EGFR and IL-6R through JAK2/STAT3 mediate epithelial-mesenchymal transition in ovarian carcinomas. *Br. J. Cancer* **100**, 134–144 (2009).
38. T. Yamauchi *et al*., Tyrosine phosphorylation of the EGF receptor by the kinase Jak2 is induced by growth hormone. *Nature* **390**, 91–96 (1997).
39. M. Steder *et al*., DNp73 exerts function in metastasis initiation by disconnecting the inhibitory role of EPLIN on IGF1R-AKT/STAT3 signaling. *Cancer Cell* **24**, 512–527 (2013).
40. M. Hedvat *et al*., The JAK2 inhibitor AZD1480 potently blocks Stat3 signaling and oncogenesis in solid tumors. *Cancer Cell* **16**, 487–497 (2009).
41. N. Zhu *et al*., ZIP restores estrogen receptor expression and response to tamoxifen in estrogen receptor negative tumors. *Biochem. Biophys. Res. Commun.* **480**, 570–573 (2016).
42. M. J. Waters, A. J. Brooks, JAK2 activation by growth hormone and other cytokines. *Biochem. J.* **466**, 1–11 (2015).
43. J. de la Rosa *et al*., A single-copy Sleeping Beauty transposon mutagenesis screen identifies new PTEN-cooperating tumor suppressor genes. *Nat. Genet.* **49**, 730–741 (2017).
44. R. Mroue, B. Huang, S. Braunstein, A. J. Firestone, J. L. Nakamura, Monoallelic loss of the imprinted gene Grb10 promotes tumor formation in irradiated Nf1+/- mice. *PLoS Genet.* **11**, e1005235 (2015).
45. E. J. Baxter *et al*.; Cancer Genome Project, Acquired mutation of the tyrosine kinase JAK2 in human myeloproliferative disorders. *Lancet* **365**, 1054–1061 (2005).
46. R. B. Riggins *et al*., Physical and functional interactions between Cas and c-Src induce tamoxifen resistance of breast cancer cells through pathways involving epidermal growth factor receptor and signal transducer and activator of transcription 5b. *Cancer Res.* **66**, 7007–7015 (2006).
47. A. Pardanani *et al*., Safety and efficacy of TG101348, a selective JAK2 inhibitor, in myelofibrosis. *J. Clin. Oncol.* **29**, 789–796 (2011).
48. S. Verstovsek, Therapeutic potential of JAK2 inhibitors. *Hematology Am. Soc. Hematol. Educ. Program* **2009**, 636–642 (2009).
49. M. B. Sonbol *et al*., Comprehensive review of JAK inhibitors in myeloproliferative neoplasms. *Ther. Adv. Hematol.* **4**, 15–35 (2013).
50. C. Gest *et al*., Ovarian cancer: Stat3, RhoA and IGF-IR as therapeutic targets. *Cancer Lett.* **317**, 207–217 (2012).
51. S. Grivennikov, M. Karin, Autocrine IL-6 signaling: A key event in tumorigenesis? *Cancer Cell* **13**, 7–9 (2008).
52. N. Benabbou *et al*., Hospicells promote upregulation of the ATP-binding cassette genes by insulin-like growth factor-I via the JAK2/STAT3 signaling pathway in an ovarian cancer cell line. *Int. J. Oncol.* **43**, 685–694 (2013).
53. S. K. Misra *et al*., Combinatorial therapy for triple negative breast cancer using hyperstar polymer-based nanoparticles. *Chem. Commun. (Camb.)* **51**, 16710–16713 (2015).
54. B. Győrffy *et al*., An online survival analysis tool to rapidly assess the effect of 22,277 genes on breast cancer prognosis using microarray data of 1,809 patients. *Breast Cancer Res. Treat.* **123**, 725–731 (2010).